Hindawi Publishing Corporation
International Journal of Digital Multimedia Broadcasting
Volume 2010, Article ID 759323, 14 pages
doi:10.1155/2010/759323

Review Article

Digital Holographic Capture and Optoelectronic Reconstruction for 3D Displays

Damien P. Kelly,[1] David S. Monaghan,[1] Nitesh Pandey,[1] Tomasz Kozacki,[2] Aneta Michałkiewicz,[2] Grzegorz Finke,[2] Bryan M. Hennelly,[1] and Malgorzata Kujawinska[2]

[1] *Department of Computer Science, National University of Ireland, Maynooth, Co. Kildare, Ireland*
[2] *Institute of Micromechanics and Photonics, Warsaw University of Technology, 8 A. Boboli St., 02525 Warsaw, Poland*

Correspondence should be addressed to Bryan M. Hennelly, bryanh@cs.nuim.ie

Received 27 April 2009; Revised 29 September 2009; Accepted 8 December 2009

Academic Editor: Georgios Triantafyllidis

The application of digital holography as a viable solution to 3D capture and display technology is examined. A review of the current state of the field is presented in which some of the major challenges involved in a digital holographic solution are highlighted. These challenges include (i) the removal of the DC and conjugate image terms, which are features of the holographic recording process, (ii) the reduction of speckle noise, a characteristic of a coherent imaging process, (iii) increasing the angular range of perspective of digital holograms (iv) and replaying captured and/or processed digital holograms using spatial light modulators. Each of these challenges are examined theoretically and several solutions are put forward. Experimental results are presented that demonstrate the validity of the theoretical solutions.

1. Introduction

3D display systems generate a great deal of public interest. The idea that any event, ranging from the trivial to the momentous, could somehow be fully recorded and the 3D scene replayed at a later time for an audience in another location is highly desirable. However, current technologies are far from this futuristic conception of 3D technology. Nevertheless recent improvements in 3D display and capture technologies have led the way for plausible pseudo-3D scenes to be recorded allowing the user to avail of a realistic 3D experience. Consider for example the development of cinema, film, TV and computer gaming over the past 30 years. Entertainment industries are constantly pushing for better 3D experiences. Whether new technologies or approaches provide a suitably realistic 3D experiences, one must consider the human perception dimension to the problem, for a more complete account we refer the reader to Chapter 17 of [1]. The consistent and continuous improvement in the quality of the sound and special effects in films is noticeably apparent. Perhaps this is even more dramatically underlined in computer gaming when one compares the improvement in graphics over the past three decades. Future improvements in 3D technology are being prepared by major players in the industry; Both Dreamworks Animation and Pixar have stated their intention to release all future films in 3D; there is an increase in the number of 3D cinemas being constructed; public screenings of 3D football matches, and so forth, are being shown in an attempt to increase public awareness of 3D technology [2]. So the question arises, how will 3D cinema translate to 3D TV?

It is a problem of content, in part, however as more people experience 3D cinema the demand for a similar 3D experience at home increases, which in turn drives the demand for 3D television content. There is a precedent for this, the changeover from black and white TV to colour TV. Several major technology companies such as Phillips and Holografika, currently have proto-types of 3D televisions that produce a convincing 3D experience. Although the current 3D technology may sometimes appear revolutionary, the fundamental science behind it is as old as film itself [3]. The central idea underpinning the 3D experience is that of stereoscopic vision [3, 4]: an observer viewing a scene sees two similar but slightly displaced versions of that scene with

the left and right eye. This information is processed by the brain and the viewer perceives a 3D scene. For a detailed introduction to some of these approaches to 3D display devices we refer the reader to [1].

Looking further into the future, another technology could potentially offer more realistic 3D capture and display: Digital Holography (DH) [5–12]. This imaging process allows the full wavefield information; amplitude and phase, to be recorded. With this information it is possible, using devices known as Spatial Light Modulators (SLM), to reconstruct the optical wavefield in another place and at another time [11–13]. Recreating the full wavefield is the only method by which an observer would be exposed to the same scene that had been recorded. While there are obstacles to achieving this goal, digital holographic capture display technology does work as shall be demonstrated by theoretical and experimental results presented in this paper.

Some of the major challenges are:

(i) the removal of the DC and conjugate image terms, which are features of the holographic recording process,

(ii) the reduction of speckle noise, a characteristic of a coherent imaging process,

(iii) increasing the angle of perspective of digital holograms, and

(iv) replaying captured and/or processed digital holograms using spatial light modulators.

In the following sections we will discuss each of these obstacles along with several different approaches that are currently being investigated to minimize their impact on image quality. While many of these issues have been addressed over the years in many different contexts, here we use a combination of these approaches in an attempt to improve holographic display techniques.

Each of the obstacles noted above must be addressed in order to capture and replay a single holographic frame. For real-time imaging however it will be necessary to capture, transmit and replay a series of frames. Real-time imaging will therefore bring challenges in additon to those already outlined. For convincing real time imaging it will be necessary to be able to replay approximately 50 frames (cinemas currently have 25 frames per second) per second. There are several potential bottlenecks to achieving this frame rate: (a) the time it takes to capture and process a frame, (b) sending data over transmission lines and finally (c) the refresh rate of the SLM devices must have a sufficiently quick to display ~50 frames per second. We note that as technology improves these timing and transmission difficulties may well recede.

In this research presented here the complex wavefield is captured in the National University of Ireland, Maynooth (NUIM), processed and transmitted to the Warsaw Technical University (WUT) where the hologram is loaded onto an SLM and reconstructed optoelectronically.

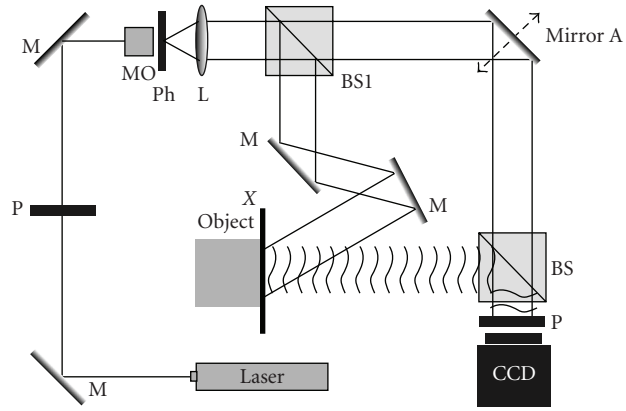

Figure 1: Schematic depicting a typical inline DH setup. M: Mirror, P: Polarizer, BS: Beam Splitter, Ph: Pinhole, and MO: Microscope Objective.

2. DC Terms and the Conjugate Image Term

In this section we examine some fundamental properties of a holographic imaging system. In Figure 1 we present a schematic of a typical DH setup. Laser light is spatially filtered using a microscope objective and a pinhole. The diverging spherical wave that emerges from the pinhole is collimated using a lens to form an approximately flat plane wave that is split into two beams, the reference beam and object beam, by the beam splitter BS1, see Figure 1. After reflection from several mirrors the object beam illuminates the object of interest. We refer to the field scattered from the object at Plane X as $u(X)$. For the remainder of the manuscript we use the space variable x to refer to the coordinate space in the capture plane and use X variable to refer to the coordinate space in the reconstruction or object plane. The object wavefield $u(X)$ now propagates to the camera face where an interference pattern between the object and the reference wavefields is formed and the resulting intensity is recorded. Using the expressions $u_z(x)$ and $u_r(x)$ to refer to the object and reference wavefields, respectively, in the camera plane we can write the resulting intensity distribution as [14–17]

$$I = |u_r(x) + u_z(x)|^2, \tag{1a}$$

$$I = I_r + I_z + u_z(x)u_r^*(x) + u_z^*(x)u_r(x), \tag{1b}$$

$$I = I_r + I_z + |u_z(x)||u_r(x)|\cos[\phi(x) - \alpha], \tag{1c}$$

where

$$u_r(x) = \exp(j\alpha), \tag{2a}$$

and where

$$u_z(x) = |u_z(x)|\exp[j\phi(x)],$$
$$u_z(x) = \sqrt{\frac{1}{j\lambda z}}\int_{-\infty}^{\infty} u(X)\exp\left[\frac{j\pi}{\lambda z}(x-X)^2\right]dX. \tag{2b}$$

We note that $I_z = |u_z(x)|^2$ and $I_r = |u_r(x)|^2$. In (2b), λ refers to the wavelength of the laser light and z, the distance between Plane X and the camera face, see Figure 1. We also note that the relationship between $u_z(x)$ and $u(X)$ defined in (2b) is the well known Fresnel transform [17]. Examining (1b) we can see that the recorded interferogram $I(x)$ contains four terms, the DC terms: I_z and I_r, the real image term: $u_z(x)u_r^*(x)$, and finally the conjugate image term, $u_z^*(x)u_r(x)$. We will assume that our reference wave is flat and therefore is constant for all values of x. This allows us to ignore the effect of the reference wave for the conjugate and real image terms as it now represents a constant phase. If we apply an inverse Fresnel transform on (1b), our image in the reconstruction plane will contain contributions from the conjugate image, the real image and the DC terms. Ideally we would like to isolate the real image term from the other terms thereby improving the quality of the reconstruction. Since the Fresnel transform is a linear operation, it is easier to understand the contribution of the different terms by considering them individually. By simulating free space propagation numerically in a computer we may back-propagate $u_z(x)$ to the object plane to recover our desired field $u(X)$. Applying an inverse Fresnel transform to the conjugate image term produces another field in the object plane which overlaps with $u(X)$, distorting the image. The DC terms, I_r and I_z will also play a negative role, distorting the reconstructed field in Plane X. We note however that if $u_r(x)$ is a flat unit amplitude plane wave, then $I_r(x)$ is constant across the capture plane and therefore is mapped by a Fourier transform to a Dirac delta function centred at zero frequency [17, 18]. This deleterious contribution may thus be filtered relatively easily using numerical techniques. Alternatively it is possible to record separately both DC terms; I_r and I_z, and to numerically subtract these from the interferogram I using a computer. In Figure 2 we present a captured and reconstructed DH of a *Starwars* character. The setup is an inline setup very similar to that depicted in Figure 1. In the experiment we use an AVT Dolphin camera with 1392 by 1048 pixels each of pitch 6.45 μm to record the interferogram while the parameters λ and z are given by $\lambda = 785$ nm, $z = 108$ mm, respectively. Performing a numerical inverse Fresnel transform on the non-processed interferogram generates the reconstructed hologram in Figure 2 [19, 20]. The DC terms and the conjugate image image noise are clearly evident. In Figure 3 we present the same reconstruction where the I_{ref} DC term has been removed using a filtering technique. We reduce the power in our object arm to a low level and ignore the contribution of the I_z term. From experimental experience we have found that this does not overly degrade the quality of the reconstructed hologram. Note the subsequent improvement in the reconstruction quality. Once the DC terms have been removed (and assuming a flat reference wave) we may rewrite (1c) as

$$I = u_z(x) + u_z^*(x) \tag{3}$$

On inspection of Figure 3, however it is clear that the conjugate image is still present and that it contributes to a significant deterioration of the reconstructed hologram. Therefore we now turn our attention to several techniques for removing this troublesome term.

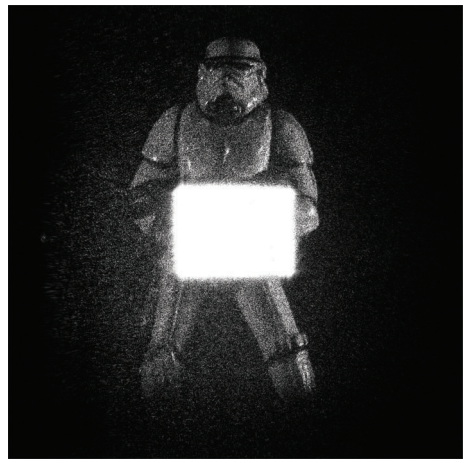

Figure 2: Reconstructed DH of a Starwars schart. Note the presence of the both the DC terms and the conjugate image term.

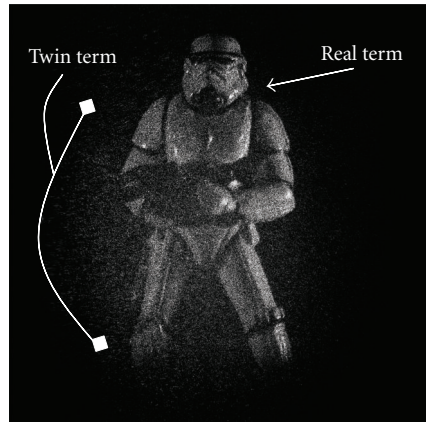

Figure 3: Same as Figure 2 however the DC terms have been removed using numerical processing techniques.

2.1. Numerical Removal of the Conjugate Image Term. Here we describe a technique for removing the conjugate image term numerically and refer the reader to [21] for a more complete description of the process. The basic idea behind this numerical conjugate image removal technique is to bring the conjugate image term into focus (where its features are sharp) and then to use edge detection techniques to remove the conjugate image term. We can achieve this by performing a forward numerical Fresnel transform on the interferogram. Performing a forward Fresnel transform on our previously captured hologram produces the result presented in Figure 4(a). Note that now the conjugate image term is in-focus. One can see by comparing Figures 2 and 4(a) that the conjugate and real image terms are inverted with respect to each other. In this particular example we wish to demonstrate the robustness of this approach. By

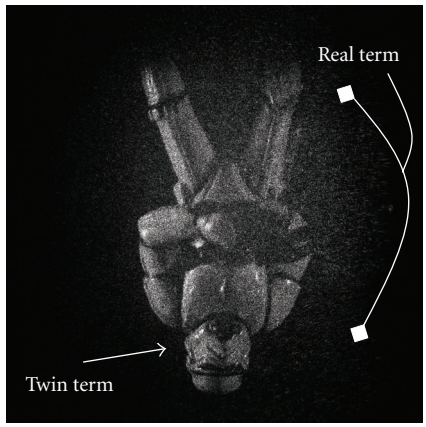

(a)

(b)

Figure 4: (a) This reconstruction is processed using the same hologram as that used to produce Figures 2 and 3. In this instance we forward propagate the hologram by a distance $+z$. In this instance the conjugate image is in focus and the real image term is out of focus. (b) This is the filter we use to remove the in-focus conjugate image.

simply setting to zero most of the in-focus term, see Figure 4(b), we may examine how much of the conjugate image has been removed. Clearly we have also removed information pertaining to the real image term; however we have attempted to discriminate more strongly against the in-focus conjugate image term. This approach can be further improved using sophisticated edge detection techniques. We now perform an inverse Fresnel transform on this processed hologram, a distance $2z$ to get back to the real image plane. In Figure 5 we present the result. While we note that the conjugate image term has not been completely removed, it has been nevertheless been significantly reduced. There are many different numerical techniques for removing the conjugate image term; see, for example, [22]. The main advantage of a numerical procedure for removing both the DC and conjugate image terms is that only one interferogram is then needed to capture our field $u(X)$. In the next section we will look at another technique for removing the conjugate

Figure 5: This reconstruction is the same as Figure 2, however both the conjugate image term and the DC terms have been removed using numerical processes described in the text.

image term that is generally more effective than the technique just described. This approach is known as phase shifting interferometric technique; however its main disadvantage is that several holograms need to be captured which may limit its application in real-time imaging [23–25].

2.2. Phase Shifting Interferometer to Remove the Conjugate Image Term. In this section we examine another technique for removing the conjugate image term. This approach, Phase Shifting Interferometry (PSI), is a technique in which the phase of one of the interfering beams in the setup is precisely changed and a set of phase shifted interferograms are recorded. These interferograms are then processed to extract the real object wavefield. In holography this means that the zero-order and the conjugate image noise can be removed. The advent of accurate piezo electric actuator technology has enabled this technique to become very useful in optical interferometry. Phase shifting applied to digital holography was applied to opaque objects by Yamaguchi and Zhang [23]. In the lab in NUIM, we have implemented controlled phase shifting to remove the zero-order and conjugate image reconstructions. A mirror (see Mirror A in Figure 1) is attached to a piezo-actuator (Piezosystem Jena, PZ38CAP) and placed in the object beam arm [23]. This mirror can be moved in a controlled and repeatable manner through very small displacements $\sim$1 nm. This allows us to introduce a controlled phase shift between the object and reference arms of the digital holographic setup. To ensure that we introduce the intended phase shift it is necessary to calibrate the piezo-actuated mirror. To perform this calibration we replace the object in Figure 1 with a plane mirror and observe the interference pattern in the camera plane. With ideal lenses and aligned optics we would expect to observe a uniform intensity pattern across the camera face. As the piezo-actuated mirror is subject to a displacement we expect the uniform intensity to vary from a maximum (when the object and reference plane waves exhibit total constructive interference) to minimum when the two beams exhibit destructive interference. We note however that with

misaligned optical elements and imperfect lenses we do not achieve this type of interference pattern. To perform our experiment we examined a region of the interferogram, summing the intensity of all the pixels therein. We then observed the variation in the intensity in this region as the piezo-actuated mirror was stepped in small increments by applying a known voltage. In Figure 6 we present the results. With this information we are now able to use PSI techniques to remove the DC and conjugate image terms. We proceed using the 4-step technique discussed by Yamaguchi et al. and capture a series of four digital holograms where the phase difference between each successive capture is $\pi/2$. From [25] we can now express the phase of the real image term as

$$\phi(x) = \frac{I_{3\pi/2} - I_{\pi/2}}{I_0 - I_\pi}, \tag{4}$$

where I_α refers to a captured hologram where the object and reference fields have been shifted α radians with respect to each other. We note that $|u_z(x)| = \sqrt{I_z}$ may be recovered by blocking the reference arm and recording the intensity of the object field. Using this procedure we can thus separate the real image term from the other contributions of the holographic imaging process. The result of reconstructing the data produced by applying (4) can be seen in Figure 7. It is interesting to compare the results presented in Figures 5 and 7. These seem to indicate that PSI-based approach yields superior results; however this should be further qualified. Capturing PSI type holograms has several significant disadvantages that may limit its application for real time imaging: (i) several captures are required, (ii) it is very important that the scene remains motionless during the entire capture process. In practice this latter constraint can be difficult to achieve and by its very nature interferometry is particularly sensitive to any type of motion. We are currently trying to improve numerical techniques for conjugate image term removal and are using PSI holograms as benchmark to determine their effectiveness.

We would to briefly comment on what is called off-axis reference holography. In this instance an off-axis plane wave is used as a reference wave. This has the effect of spatially separating the real and conjugate image so that the two terms may be isolated and separated from each other using numerical techniques. This technique has application for real-time imaging application, [26, 27]; however it imposes restrictive constraints on the recording device. Recording using an off-axis architecture may reduce the spatial resolution of the resulting hologram by up to four fold in contrast with an inline approach. For this reason we concentrate primarily on inline recording setups in this manuscript.

3. Speckle Noise Reduction

When light that is fairly coherent (both temporally and spatially) is reflected from an optically rough surface, the resulting intensity pattern has a random spatial intensity variation. This is known as speckle pattern. Although one of the first observations of the speckle phenomenon was made by Exner in 1878 and discussed widely at the time in the literature, it was the invention of the laser that led researchers to "re-discover" speckle in the 1960s. As lasers became more widely available, the speckle effect was soon put to good use in nondestructive, noncontact metrology applications. Nevertheless speckle is a significant hindrance in imaging applications and acts to severely degrade the performance of coherent optical systems. For imaging applications, particularly those that involve display or projection systems, the effect is striking, uncomfortable and irritating due in large part to the high contrast (unity contrast) associated with a speckle distributions. Thus speckle is both a fundamental property of a coherent imaging process and a significant hindrance for imaging applications. Over the years many different techniques for reducing speckle have been developed, unfortunately however these techniques

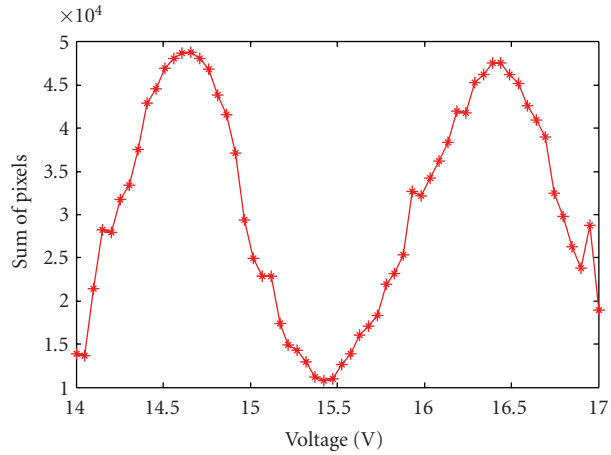

Figure 6: Calibration curve for PiezoJena actuator (Piezosystem Jena, PZ38CAP) driven using controller: NV401CLE. The intensity varies from a maximum at ~14.6 V, to a minimum at ~15.5 V, corresponding to a $\pi/2$ phase shift.

Figure 7: This reconstruction is the same as Figure 5, where both the conjugate image term and the DC terms have been removed. Unlike in the numerical procedure used in Figure 5, we have applied a PSI technique to separate out the real image term.

tend to reduce the resolution of the imaging system [28–30]. For example we have examined using mean filtering to reduce the appearance of speckles in reconstructed digital holograms. This approach reduces the speckle contrast at the expense of effectively low-pass filtering our image. There is therefore a corresponding reduction in higher spatial frequency content. Alternatively if several speckle fields are summed on an intensity basis the speckle contrast can be reduced significantly, see for example the discussion in Chapter 5 of [29]. It is of fundamental importance to realise that speckle fields added on a complex amplitude basis will not reduce the speckle contrast [30], they must be added on an intensity basis. Calculating the expected reduction in speckle contrast by summing different speckle fields on an intensity basis requires an involved theoretical investigation into the statistical temporal and spatial correlations between each of the different speckle intensity patterns. Furthermore, if the device detecting these intensity fields spatially and temporally integrates the instantaneous intensity, then the statistical properties of integrated speckle fields must also be considered. Again we refer the reader to [29] for more detail. However a good rule of thumb as to the expected reduction in speckle contrast is given by assuming that the speckle intensity patterns are statistically independent. With this assumption the speckle contrast, C is given by

$$C = \frac{1}{\sqrt{N}}, \tag{5}$$

where N is the number of statistically independent speckle intensity patterns.

In this section, we are going to examine two different approaches to speckle reduction. We will first examine how to reduce speckle using convenient numerical techniques before examining how to reduce speckle by capturing multiple holograms of the same scene.

3.1. A Numerical Approach to Speckle Reduction. Here we investigate a numerical technique for reducing the speckle contrast in a reconstructed digital hologram. We do this by summing together multiple intensity images, each of which contains a statistically independent speckle pattern lying on top of an unchanging object intensity distribution. Therefore from one captured hologram we need to somehow generate a relatively constant object intensity distribution and several statistically independent speckle fields. To do this we adopt a digital version [31] of an old technique proposed in the 1970's by Dainty and Welford [32], where the Fourier transform of the hologram is repeatedly spatially filtered and the resulting intensities are added together. Each spatial filter corresponds to a different rectangular band in the frequency domain. By moving the spatial filter in the Fourier domain we allow different parts of the hologram's Fourier spectrum to contribute to the holographic reconstruction. We note that by removing spatial frequencies we will reduce the resolution of our reconstructed hologram, however we will also reduce the speckle contrast in the reconstructed image. In Figure 8 we present our results. Figure 8(a) is the reconstructed hologram resulting from one intensity from only a single bandpass filter. This bandpass filter corresponds to a 348×348 pixel region in the frequency domain. In Figures 8(b)–8(f) we show the resulting image when 1, 3, 5, 7, 10 and 14 band pass filtering operations have been performed and the resulting intensities have been averaged. It is clear from examining Figure 8 that while the speckle contrast has been reduced it comes with the price of reducing the spatial resolution of the reconstructed image.

It is noticeable that in Figure 8(a) we clearly see dark horizontal and vertical fringes that overly the image of the object. These unwanted terms are due to the square bandpass filtering operation that created this image. Multiplication with a displaced rectangular function (one quarter the bandwidth of the fully reconstructed image) in the frequency domain amounts to convolution with a Sinc function [18] in the image plane. Furthermore this Sinc function is multiplied by a linear phase factor that relates to the displacement of the rectangular function. Convolution of the fully reconstructed image with this tilted Sinc function brings about the dark horizontal and vertical fringes that are shown in Figure 8(a). As we add together the intensities of different bandpassed versions of the image these fringes are averaged away since they are different for each bandpass. In Figure 8(b), after three filtered image intensities have been added together it is observed that the horizontal fringes have been visibly reduced but the vertical one remains in the image. This is due to the fact that the three bandpass filters were located vertically with respect to one another in the frequency domain. In Figure 8(c) after five intensities are added we see some reduction in the vertical fringe. This is due to the fact that the five band pass filters were composed of a column of four vertically shifted rectangular functions of size 348×348 pixels. For the fifth bandpass filter we move horizontally to the next column. This latter filter brings about the reduction in the vertical filter. As we move across all the columns and rows all the fringes are reduced.

3.2. A Multiple Capture Approach to Speckle Reduction. We note that the addition of the intensity of multiple hologram reconstructions has been previously demonstrated in the literature [33–37]. In [33] the illuminating source was rotated between captures in order to generate a series of reconstructions of the same static object with statistically independent speckle noise terms. The superposition of the intensity profiles reinforces the object image while the overlying speckle noise is averaged away. In [34] a similar method is used, this time the wavelength of the source is varied between captures. In [35] the angle of incidence upon the object of the illuminating source is varied between captures and in [36] a random diffuser, placed just after the source illuminating the object, is moved between captures. In [37] the authors set out to improve a Fourier Digital holography metrology system. The unwrapped phase (showing deformation topology) is averaged for multiple captures where there is a slight change in the CCD position between captures.

In our experiment, we introduce a piece of frosted glass (diffuser) into the object arm of our digital holographic setup. Standard PSI techniques are used to remove the DC and conjugate image terms. We are able to illuminate our

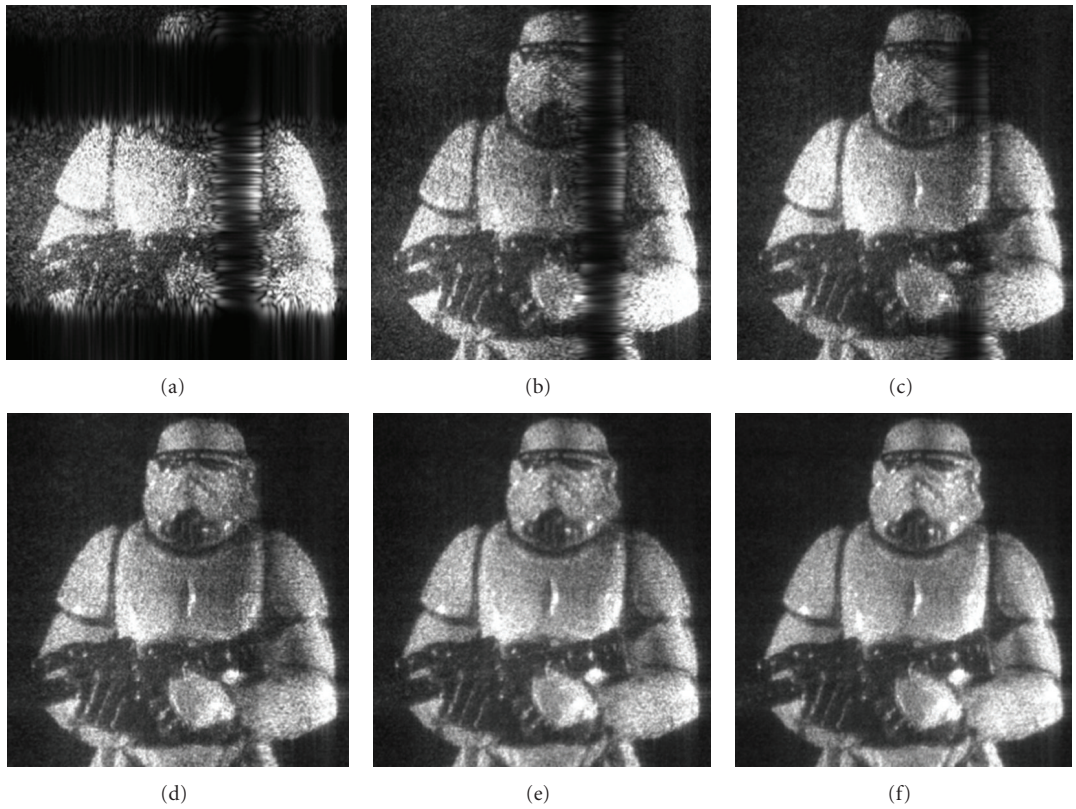

(a) (b) (c)

(d) (e) (f)

Figure 8: Removal of speckle noise using a numerical technique discussed in the text. We generate 14 different reconstructions from 1 hologram by filtering in the Fourier domain with a square aperture window of size 128 by 128 pixels. (a) One image, (b) Sum of 3 intensities, (c) Sum of 5 intensities, (d) Sum of 7 intensities, (e) Sum of 10 intensities, (f) Sum of 14 intensities.

object with a random diffuse field which is then translated approximately 5 mm between captures. This is similar to the approach that is presented in [36]. However we note that in [36] the off axis architecture was employed to record the holograms and in the results here an in-line PSI method was used. We believe that this may be the first time that a moving diffuser has been employed to reduce the speckle from PSI reconstructed holograms. One of the captured PSI holograms was reconstructed and is presented in Figure 9(a). The reconstruction is contaminated by speckle noise. We now move the piece of frosted glass and illuminate our object with a statistically different random diffuse field. Another PSI hologram is captured, reconstructed and added to Figure 9(a) on an intensity basis. Note that while speckle contrast has been reduced the resolution of the reconstructed hologram has been unaffected unlike in Figures 8(a)–8(f). A series of holograms were captured in a similar manner and the results are displayed in Figures 9(a)–9(f).

4. Increasing Perspective of DH Using a Synthetic Aperture Technique

Recently there has been growing interest in the use of Synthetic Aperture (SA) methods in order to increase the effective aperture of the recording CCD [38–44]. This in turn may allow one to generate a reconstructed image with a higher resolution [39], although we do not demonstrate this effect in this paper, and also to generate reconstructions showing a much greater range of perspective in the third dimension. SA digital holography may offer the greatest potential to record digital holograms that show sufficient 3D perspective for commercial display. In general all of the methods appearing in the literature aim to capture multiple holograms, each corresponding to a different section of the object wavefield. These can then be somehow merged together in order to obtain a larger hologram. The larger hologram will allow for a greater range of perspective to be seen as we reconstruct different windows of our SA hologram.

In [42], a method was outlined in which multiple holograms are recorded where the object is rotated between captures. The angle of rotation is small so that (i) the hologram appearing on the CCD does not decorrelate and (ii) some area of the wavefield appearing on the CCD is common to both captures. This allows correlation techniques to be used to determine accurately the change in angle between captures. Stitching is then performed in the Fourier domain to create a larger hologram. We are currently developing a variant of this method in which we place a mirror between the illuminated object and the CCD. It is the mirror that is rotated in our set-up meaning that we do not have to worry about speckle decorrelation that

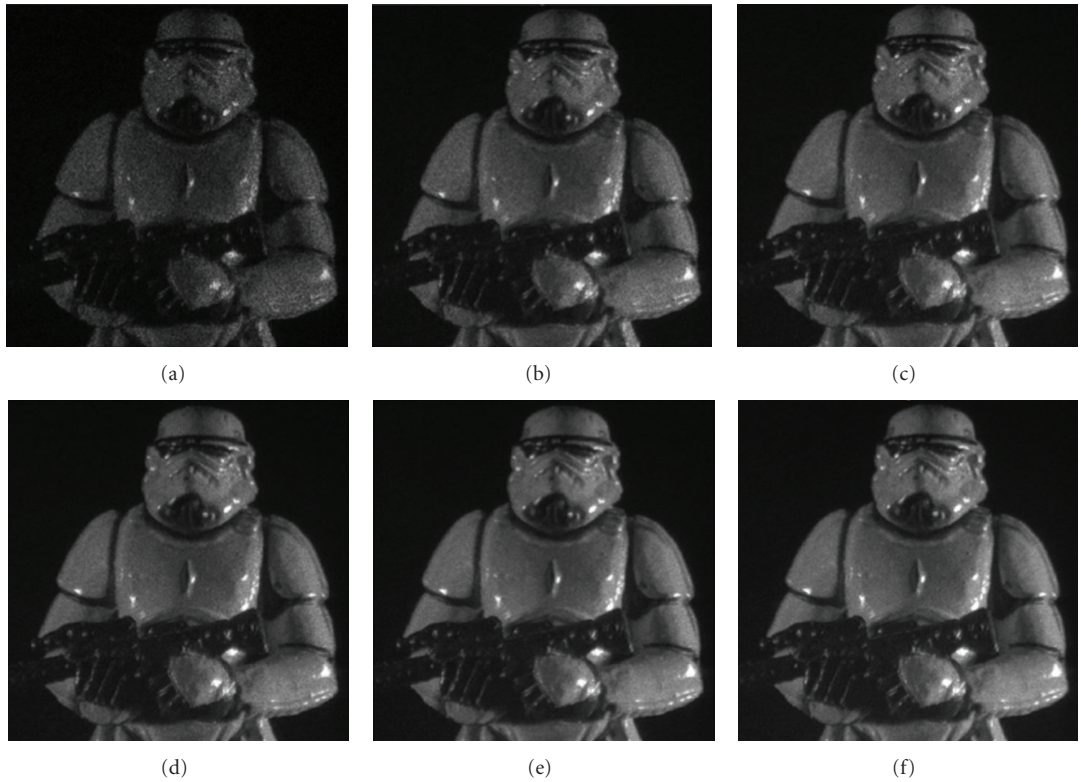

Figure 9: Removal of speckle noise by adding multiple reconstructed digital hologram captures together on an intensity basis. For each capture a different diffuse and random field is used to illuminate our object. (a) One image, (b) Sum of 3 intensities, (c) Sum of 5 intensities, (d) Sum of 7 intensities, (e) Sum of 10 intensities, (f) Sum of 14 intensities.

arises due to rotation of the object. However, the mirror creates the need for a correlation and stitching in the spatial domain. Therefore, we stitch our holograms together in four dimensions, in space (x and y) and spatial frequency (f_x and f_y). The shift between the two discrete hologram matrices is resolved to subpixel accuracy. We do this by applying a phase shift (corresponding to less than the pixel size, e.g., 1/5th of the pixel size) to one of the matrices in the Fourier domain. Since a phase shift in the Fourier domain corresponds to a shift in space in the space domain the matrix is said to be subpixel shifted in the space domain. This is equivalent to interpolating the discrete object wavefield "in-between" the pixels. We perform the correlations on each such subpixel shifted matrix and identify the best shifted matrix which gives the highest correlation peak value. This is further done for different values of the subpixel shift, for example, (1/5th of pixel, 1/8th of pixel, etc.). The best shift d is chosen and thus resolved to subpixel accuracy. The steps taken for stitching are described in the schematic in Figure 10. We refer the reader to [42] for a thorough analysis of the method.

In Figures 11 and 12 we show some preliminary results. In Figure 11 we show a digital hologram of a resolution chart and the reconstruction. In Figure 12, we capture five holograms of the same static object, while rotating a mirror in the set-up. Each new hologram allows us to add approximately 300 new pixels to the hologram. In future work we expect to use this method to record 3D macroscopic objects with a range of perspective of approximately 10–15 degrees.

5. Optical Reconstruction of Digital Holograms Using with a Liquid Crystal Spatial Light Modulator

As we have seen in the previous sections in order to inspect the visual information encoded in a digital hologram we can apply numerical reconstruction algorithms. While this approach is suitable for many different applications, in particular metrology or microscopy, it is not appropriate for 3D display systems. If we wish to view the hologram in real 3D space, then the information contained in the digital hologram must be replayed using optoelectronic techniques. Briefly, some of the information contained in the captured hologram is loaded onto an SLM device. A plane wave is then reflected off the surface of the device, and an approximation to the original object wavefield is created. In our display system we use a reflective liquid crystal Spatial Light Modulator (SLM): HoloEye (model: HEO 1080 P) with 1920×1080 pixels, each with a pitch of $\Delta_{\text{rec}} = 8\,\mu\text{m}$ to approximately reconstruct the original object wavefield optically. A single SLM allows us to display either a phase (phase mode) or an amplitude (amplitude

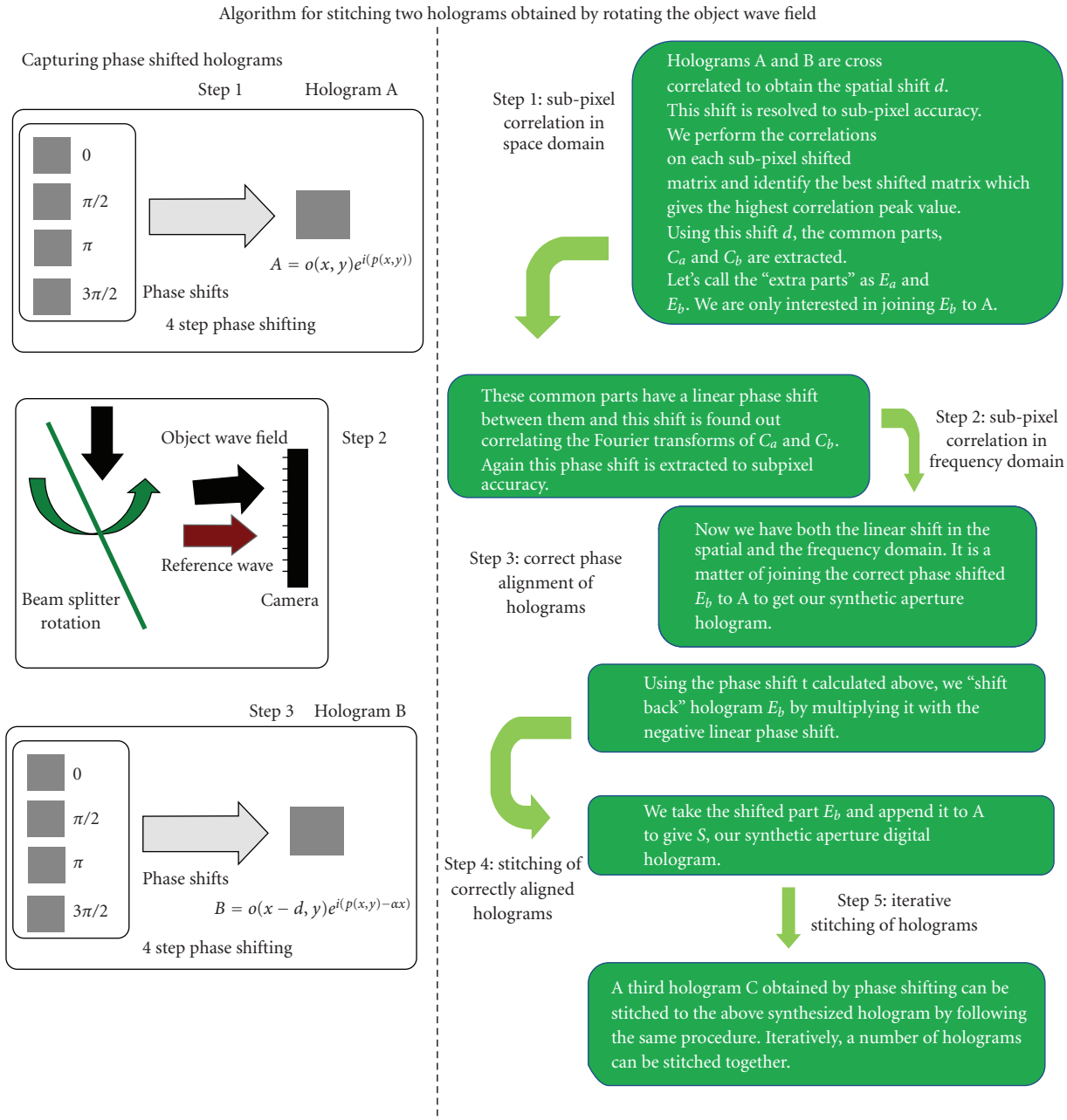

Figure 10: Schematic showing the various steps taken in the stitching process. The beam splitter in Step 2 on the left-hand side corresponds to BS in Figure 1. It is rotated in order to rotate the object wave field.

mode) distribution. Displaying both amplitude and phase is not straight-forward, as two modulators working in different modes (amplitude or phase) are required. These two SLM's would then need to be carefully aligned and furthermore would also be very sensitive to errors introduced by relative mechanical motions or vibrations between these two devices. Also, whether we use amplitude or phase mode depends on the data we load onto our SLM. We note for example that an actual interferogram (our unprocessed digital holograms that are captured in NUIM) contain only real positive numbers and therefore can be replayed using our SLM in amplitude mode. As we shall see however the resulting optoelectronic reconstruction is contaminated by both the DC terms and the conjugate image term. If we use numerical techniques to process our hologram, thereby obtaining the complex field information associated with our object distribution, we obtain both amplitude and phase data. For the alignment issues identified above we must now opt to load either the phase or amplitude data onto our SLM. From experimental experience we have found that more convincing optical reconstructions are obtained when the phase data is loaded onto our SLM and the device is operated in phase mode only, see also [17, Section 9.9.3]. Before we turn our attention to discussing some of our experimental

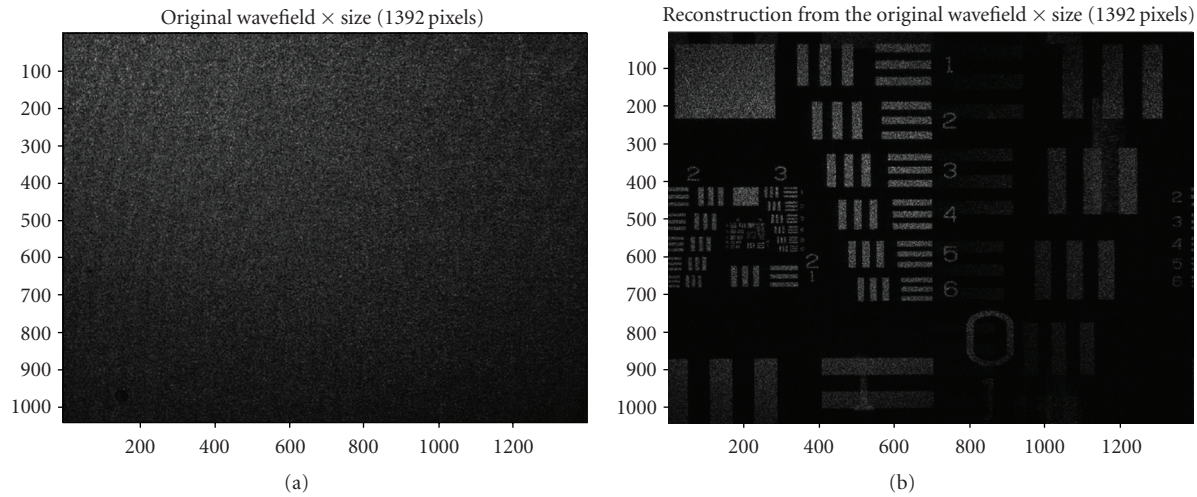

Figure 11: (a) Amplitude of a PSI hologram of a transparent USAF resolution chart having been illuminated through a diffuser. The hologram has 1040 × 1392 pixels. In (b) we show the reconstruction of the digital hologram.

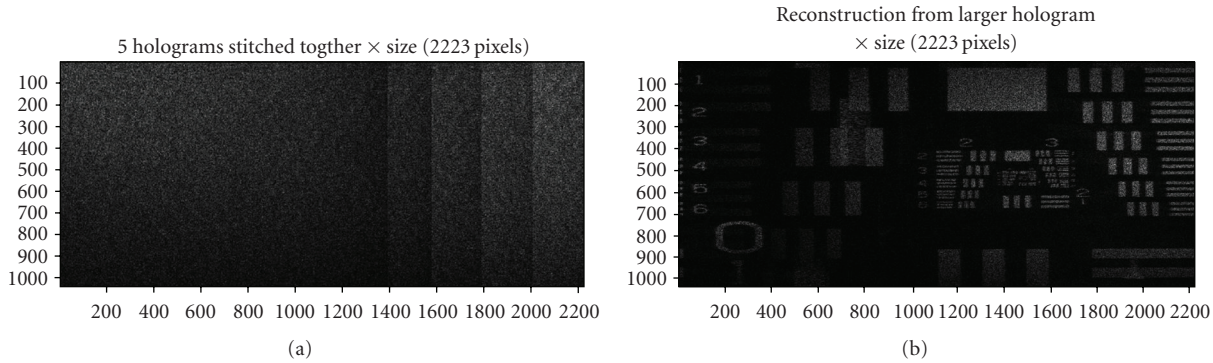

Figure 12: (a) Amplitude of a Synthetic Aperture digital hologram. Five recordings have been stitched together. The resultant hologram has clear discontinuities that would not be visible in the ideal case. Stitching has also been implemented in the spatial frequency domain. Approximately 300 pixels are added with each addition capture. The SA DH has 2223 pixels in the x direction. In (b) we show the reconstruction of SA DH.

results, we note that the camera used by NUIM to capture the original hologram has 1392 × 1048 pixels, with a pixel pitch $\Delta_{\text{reg}} = 6.45\,\mu$m. The mismatch between the dimensions of captured hologram and our replay device (see Section 2) effects optical reconstruction in two ways: (i) It modifies the distance of reconstruction plane to SLM plane according to the following formula:

$$z_{\text{rec}} = z_{\text{reg}} \frac{\lambda_{\text{reg}} \Delta_{\text{rec}}^2}{\lambda_{\text{rec}} \Delta_{\text{reg}}^2}, \tag{6a}$$

where the z_{reg} is the distance between detector and object planes, and (ii) A transverse magnification of

$$M = \frac{\Delta_{\text{rec}}}{\Delta_{\text{reg}}}, \tag{6b}$$

is now introduced to the reconstruction image. In Figure 13 we present a schematic to illustrate the physical optical setup that is used by WUT to optoelectronically reconstruct the captured holograms. We note that the wavelengths used to capture the original wavefield and the wavelength used for reconstruction differ, that is, $\lambda_{\text{rec}} = 532$ nm, while $\lambda_{\text{reg}} = 785$ nm. Using (6a) and (6b) we thus find that $z_{\text{rec}} = 281.48$, $z_{\text{reg}} = 638.95$ mm and $M = 1.24$. In Figure 14 we present an optoelectronic reconstruction of the captured digital hologram that was used to generate Figure 2. Since this unprocessed hologram is real, it could be replayed using a single SLM operating in amplitude mode. Experimentally however we have found that a good optical reconstruction, with a higher diffraction efficiency, is obtained when we use our SLM in phase mode and refer the reader to Sections 4.4.3 and 4.4.4 of [17] for a more complete discussion of this issue. This behavior has also been verified with some preliminary numerical simulations. One of the most disturbing terms in our optoelectronic reconstruction is the I_{ref} DC term, see (1a)–(1c) and Figure 14, which can be removed numerically. The DC term covers valuable space of the holographic display. This is especially significant since SLM devices have limited viewing angles ($\sim 2^\circ$) and the majority of the reconstructed image will be located within

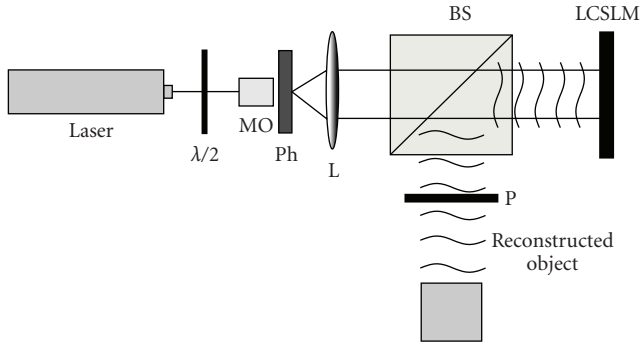

Figure 13: Scheme of setup for optical reconstruction with SLM, P: Polarizer, BS: Beam Splitter, Ph: Pinhole, and MO: Microscope Objective, L: Collimator lens, $\lambda/2$: Half-Wave Plate.

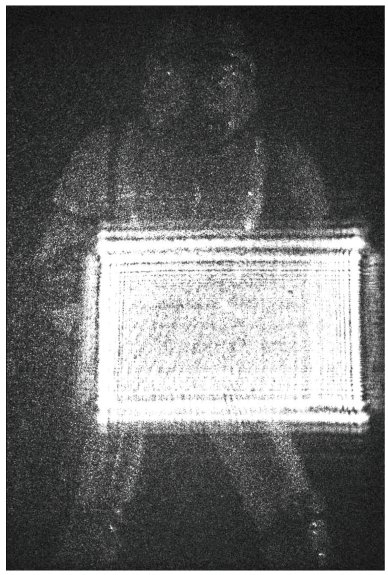

Figure 14: Optical reconstruction of holographic data with SLM: reconstruction of intensity hologram.

the zero order area, again we refer the reader to Figure 14. Also we have found that the DC term removal is especially significant for holographic reconstructions at small distances or for reconstructions of specimens with fine features.

We now turn our attention to removing the DC terms and the conjugate image term. In Section 2 we have presented two techniques for extracting the real image term from the hologram. In Section 2.1 we have presented numerical method of filtering the object field from a single hologram. The application of the method on a hologram gives us an approximation to the real image term; some features of the object field are filtered as well as the twin image term. After processing our hologram we obtain the complex information associated with the object wavefield. As we have previously noted we now discard the amplitude information displaying only the phase data on our SLM. The result of optoelectronic holographic reconstruction is presented in Figure 15(a).

Estimating our real object field can be achieved more accurately using PSI techniques, as discussed in Section 2.2. Ideally the PSI technique returns the exact object field. Errors can be introduced due to system instability during the capture or the phase step error. In Section 2.2 we used the four frames PSI technique to recover our object field. In Figure 15(b) optoelectronic reconstruction from phase of real holographic image obtained with PSI technique is presented.

Another disturbing feature of holographic imaging technique is speckle noise. Section 3 presents a review of methods that can be used to reduce this speckle noise. The most promising is a multiple capture approach to speckle reduction. Here we apply this technique to our optoelectronic reconstruction. For our numerical reconstructions, the processing and propagation of our holograms are performed numerically. Finally the calculated intensity distributions are added together. Here however the last two steps (propagation and intensity summation) are performed optically by diffraction and then by an intensity detector, that is, our eyes or the camera we use to image our optical reconstruction. We use set of ten real object waves, filtered using our PSI technique, as described in Section 3.2. These ten phase distributions were loaded sequentially onto our SLM, at a refresh rate of 60 Hz, in a continuous manner. By adjusting the exposure time of our camera we get the CCD to average (integrate) the intensity distributions of all 10 images. The result is presented in Figure 16. Figure 16(a) shows the optoelectronic reconstruction from a single hologram, while Figure 16(b) is the reconstruction obtained from ten image set. It is clearly visible that the speckle pattern has been significantly suppressed demonstrating the usefulness of this approach for optoelectronic reconstruction.

As noted previously the spatial resolution of digital holograms may be increased using SA techniques. In Figure 17 we present some preliminary experimental results. Using SA techniques we captured a series of digital holograms that were then stitched together, see Section 4 to form a larger hologram. A section of this hologram was then selected and displayed on the SLM. When replayed optoelectronically it produces the result shown in Figure 17(a). A different section of the hologram was then loaded onto the SLM and replayed to produce Figure 17(b).

6. Conclusion

In this manuscript we have examined the feasibility of using digital holographic techniques to record and replay 3D scenes. We have investigated some fundamental difficulties associated with this imaging technique and suggested several theoretical solutions to overcome them. We have demonstrated the effectiveness of our solutions with experimental results. In Section 2 we examined how to remove the DC and conjugate image terms that arise due to the holographic recording process using a numerical approach and a multiple capture approach based on Phase Shifting Interferometry. In Section 3 we focused on eliminating/reducing the disturbing effect of speckle so as to minimize its negative impact on image quality. Two different approaches were again discussed, one numerical and another based on a multiple

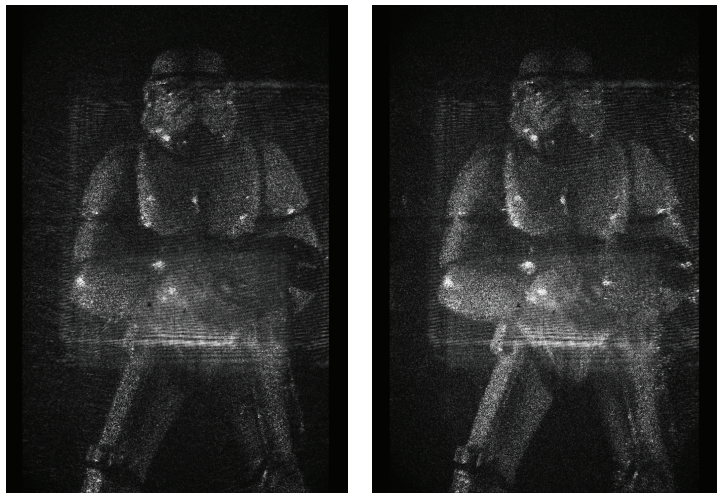

(a) (b)

Figure 15: Optoelectronic reconstruction from phase of real object beam obtained with: (a) numerical method of real object beam filtering from single hologram, (b) 4 frames PSI technique of real object beam filtering.

(a) (b)

Figure 16: Removal of speckle noise in optoelectronic reconstruction by CCD integration of reconstructed images: (a) reconstruction from one image, (b) reconstruction from ten images.

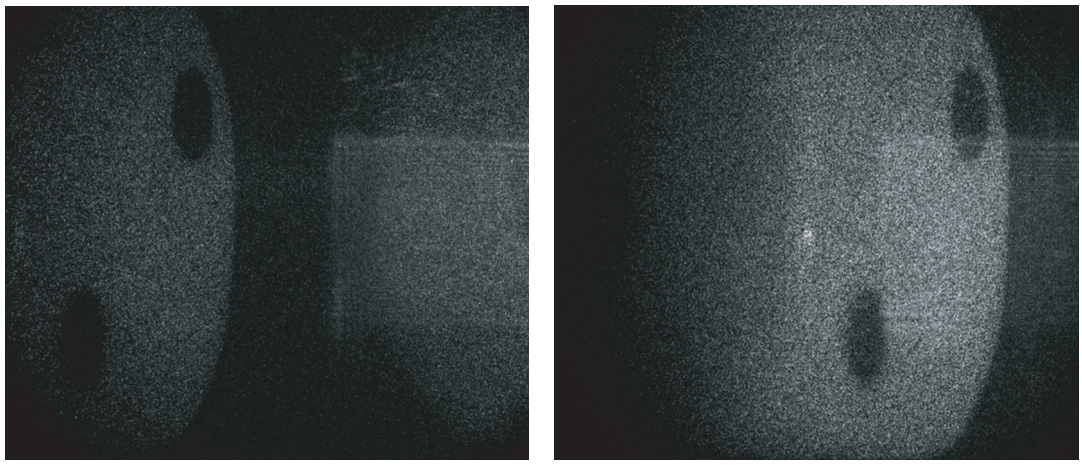

Figure 17: Reconstruction of synthetic aperture hologram.

capture technique. We do note that there are many other techniques for reducing speckle which we are continuing to investigate. In Section 4 we attempted to address the limited angular perspective of digital holograms using a synthetic aperture approach. Multiple holograms, slightly displaced from each other were recorded and stitched together using numerical techniques that we have developed. Finally in Section 5 we examined the replay or display of digital holograms using liquid crystal Spatial Light Modulators (SLM). We demonstrated experimentally that it is possible to optoelectronically replay digital holograms in one location (Poland) that have been captured elsewhere (Ireland). We have replayed synthetic aperture holograms, experimentally demonstrating the increased perspective that follows from this approach for the first time. We hope to shortly investigate the live broadcasting of 3D scenes from Ireland to Poland which may also have applications in metrology [45].

Much work remains to be done. We envisage a continued improvement in both CCD cameras and their pixel count which is essential for capturing high resolution digital holograms. We also expect to see continual improvements in spatial light modulators, both their pixel count and their ease of use and flexibility. From this collaborative research exercise we can conclude that while several major obstacles still stand in the way of real-time holographic capture and display systems, a lot of these issues will become less significant as current SLM and CCD/CMOS technologies improve. In the design of future 3D systems it will be essential to consider how the human perception effects the quality of the 3D experience. Already there are preliminary investigations underway [46]. Improvements in these areas will dramatically alter the landscape perhaps making digital holography a more feasible approach for future 3D display and capture systems.

Acknowledgment

This research is funded from the European Community's Seventh Framework Programme FP7/2007 2013 under Grant agreement 216105 "Real 3D."

References

[1] H. M. Ozaktas and L. Onural, *Three-Dimensional Television*, Springer, Berlin, Germany, 2008.

[2] R. Millman, "3D digital imax cinemas open for business," December 2008.

[3] N. A. Dodgson, "Autostereoscopic 3D displays," *Computer*, vol. 38, no. 8, pp. 31–36, 2005.

[4] N. A. Dodgson, "Analysis of the viewing zone of the Cambridge autostereoscopic display," *Applied Optics*, vol. 35, no. 10, pp. 1705–1710, 1996.

[5] D. Gabor, "A new microscopic principle," *Nature*, vol. 161, no. 4098, pp. 777–778, 1948.

[6] T. M. Kreis, M. Adams, and W. P. O. Jüptner, "Methods of digital holography: a comparison," in *Optical Inspection and Micromeasurements II*, vol. 3098 of *Proceedings of SPIE*, pp. 224–233, Munich, Germany, June 1997.

[7] T. M. Kreis, "Frequency analysis of digital holography," *Optical Engineering*, vol. 41, no. 4, pp. 771–778, 2002.

[8] T. M. Kreis, "Frequency analysis of digital holography with reconstruction by convolution," *Optical Engineering*, vol. 41, no. 8, pp. 1829–1839, 2002.

[9] T. M. Kreis and W. P. O. Jüptner, "Suppression of the DC term in digital holography," *Optical Engineering*, vol. 36, no. 8, pp. 2357–2360, 1997.

[10] D. P. Kelly, B. M. Hennelly, N. Pandey, T. J. Naughton, and W. T. Rhodes, "Resolution limits in practical digital holographic systems," *Optical Engineering*, vol. 48, no. 9, Article ID 095801, 13 pages, 2009.

[11] A. Michalkiewicz, M. Kujawinska, J. Krezel, L. Sałbut, X. Wang, and P. J. Bos, "Phase manipulation and optoelectronic reconstruction of digital holograms by means of LCOS spatial light modulator," in *Eighth International Symposium on Laser Metrology*, vol. 5776 of *Proceedings of SPIE*, pp. 144–152, Merida, Mexico, February 2005.

[12] U. Gopinathan, D. S. Monaghan, B. M. Hennelly, et al., "A projection system for real world three-dimensional objects using spatial light modulators," *Journal of Display Technology*, vol. 4, no. 2, pp. 254–261, 2008.

[13] D. S. Monaghan, U. Gopinathan, D. P. Kelly, T. J. Naughton, and J. T. Sheridan, "Systematic errors of an optical encryption system due to the discrete values of a spatial light modulator," *Optical Engineering*, vol. 48, Article ID 027001, 7 pages, 2009.

[14] O. Schnars and W. P. Jüptner, "Direct recording of holograms by a CCD target and numerical reconstruction," *Applied Optics*, vol. 33, no. 2, pp. 179–181, 1994.

[15] U. Schnars and W. P. Jüptner, "Digital recording and numerical reconstruction of holograms," *Measurement Science and Technology*, vol. 13, no. 9, pp. R85–R101, 2002.

[16] U. Schnars and W. P. Jüptner, *Digital Holography: Digital Recording, Numerical Reconstruction and Related Techniques*, Springer, Berlin, Germany, 2005.

[17] J. Goodman, *Introduction to Fourier Optics*, McGraw-Hill, New York, NY, USA, 2nd edition, 1966.

[18] R. Bracewell, *The Fourier Transform and Its Applications*, McGraw-Hill, New York, NY, USA, 1965.

[19] D. P. Kelly, B. M. Hennelly, W. T. Rhodes, and J. T. Sheridan, "Analytical and numerical analysis of linear optical systems," *Optical Engineering*, vol. 45, no. 8, Article ID 088201, 12 pages, 2006.

[20] B. M. Hennelly and J. T. Sheridan, "Generalizing, optimizing, and inventing numerical algorithms for the fractional Fourier, Fresnel, and linear canonical transforms," *Journal of the Optical Society of America A*, vol. 22, no. 5, pp. 917–927, 2005.

[21] C. McElhinney, B. M. Hennelly, L. Ahrenberg, and T. J. Naughton, "Removing the twin image in digital holography by segmented filtering of in-focus twin image," in *Optics and Photonics for Information Processing II*, vol. 7072 of *Proceedings of SPIE*, San Diego, Calif, USA, August 2008.

[22] T. Latychevskaia and H.-W. Fink, "Solution to the twin image problem in holography," *Physical Review Letters*, vol. 98, no. 23, Article ID 233901, 4 pages, 2007.

[23] I. Yamaguchi and T. Zhang, "Phase-shifting digital holography," *Optics Letters*, vol. 22, no. 16, pp. 1268–1270, 1997.

[24] Y.-Y. Cheng and J. C. Wyant, "Phase shifter calibration in phase-shifting interferometry," *Applied Optics*, vol. 24, pp. 3049–3052, 1985.

[25] I. Yamaguchi, J.-I. Kato, S. Ohta, and J. Mizuno, "Image formation in phase-shifting digital holography and applications to microscopy," *Applied Optics*, vol. 40, no. 34, pp. 6177–6186, 2001.

[26] T. Colomb, F. Montfort, J. Kühn, et al., "Numerical parametric lens for shifting, magnification, and complete aberration compensation in digital holographic microscopy," *Journal of the Optical Society of America A*, vol. 23, no. 12, pp. 3177–3190, 2006.

[27] S. Grilli, P. Ferraro, S. De Nicola, A. Finizio, G. Pierattini, and R. Meucci, "Whole optical wavefields reconstruction by digital holography," *Optics Express*, vol. 9, no. 6, pp. 294–302, 2001.

[28] J. W. Goodman, *Statistical Optics*, John Wiley & Sons, New York, NY, USA, 1985.

[29] J. W. Goodman, *Speckle Phenomena in Optics*, Roberts, Englewood, Colo, USA, 2007.

[30] J. W. Goodman, "Some fundamental properties of speckle," *Journal of the Optical Society of America*, vol. 66, pp. 1145–1150, 1976.

[31] J. Maycock, B. M. Hennelly, J. B. McDonald, et al., "Reduction of speckle in digital holography by discrete Fourier filtering," *Journal of the Optical Society of America A*, vol. 24, no. 6, pp. 1617–1622, 2007.

[32] J. C. Dainty and W. T. Welford, "Reduction of speckle in image plane hologram reconstruction by moving pupils," *Optics Communications*, vol. 3, no. 5, pp. 289–294, 1971.

[33] X. Kang, "An effective method for reducing speckle noise in digital holography," *Chinese Optics Letters*, vol. 6, no. 2, pp. 100–103, 2008.

[34] T. Nomura, M. Okamura, E. Nitanai, and T. Numata, "Image quality improvement of digital holography by superposition of reconstructed images obtained by multiple wavelengths," *Applied Optics*, vol. 47, no. 19, pp. D38–D43, 2008.

[35] L. Ma, H. Wang, W. Jin, and H. Jin, "Reduction of speckle noise in the reconstructed image of digital hologram," in *Holography and Diffractive Optics III*, vol. 6832 of *Proceedings of SPIE*, Beijing, China, November 2008.

[36] J. Garcia-Sucerquia, J. H. Herrera Ramírez, and R. Castaneda, "Incoherent recovering of the spatial resolution in digital holography," *Optics Communications*, vol. 260, no. 1, pp. 62–67, 2006.

[37] T. Baumbach, E. Kolenović, V. Kebbel, and W. Jüptner, "Improvement of accuracy in digital holography by use of multiple holograms," *Applied Optics*, vol. 45, no. 24, pp. 6077–6085, 2006.

[38] L. Martínez-León and B. Javidi, "Synthetic aperture single-exposure on-axis digital holography," *Optics Express*, vol. 16, no. 1, pp. 161–169, 2008.

[39] V. Mico, Z. Zalevsky, P. García-Martínez, and J. García, "Synthetic aperture superresolution with multiple off-axis holograms," *Journal of the Optical Society of America A*, vol. 23, no. 12, pp. 3162–3170, 2006.

[40] F. Le Clerc, M. Gross, and L. Collot, "Synthetic-aperture experiment in the visible with on-axis digital heterodyne holography," *Optics Letters*, vol. 26, no. 20, pp. 1550–1552, 2001.

[41] R. Binet, J. Colineau, and J.-C. Lehureau, "Short-range synthetic aperture imaging at 633 nm by digital holography," *Applied Optics*, vol. 41, no. 23, pp. 4775–4782, 2002.

[42] B. M. Hennelly, T. J. Naughton, J. B. McDonald, Y. Frauel, and B. Javidi, "A method for superresolution in digital holography," in *Optical Information Systems IV*, vol. 6311 of *Proceedings of SPIE*, San Diego, Calif, USA, August 2006.

[43] J. H. Massig, "Digital off-axis holography with a synthetic aperture," *Optics Letters*, vol. 27, no. 24, pp. 2179–2181, 2002.

[44] C. Yuan, H. Zhai, and H. Liu, "Angular multiplexing in pulsed digital holography for aperture synthesis," *Optics Letters*, vol. 33, no. 20, pp. 2356–2358, 2008.

[45] W. Osten, T. Baumbach, and W. Jüptner, "Comparative digital holography," *Optics Letters*, vol. 27, no. 20, pp. 1764–1766, 2002.

[46] T. M. Lehtimäki, K. Sääskilahti, R. Näsänen, and T. J. Naughton, "Visual perception of digital holograms on autostereoscopic displays," in *Three-Dimensional Imaging, Visualization, and Display*, vol. 7329 of *Proceedings of SPIE*, Orlando, Fla, USA, April 2009.